

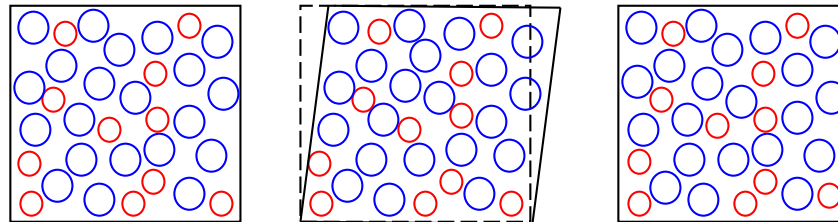
# Atomistic modeling of cyclic loading and heat treatment processes for tuning the mechanical properties of amorphous alloys

Nikolai V. Priezjev

Department of Mechanical and Materials Engineering

Wright State University

Movies, preprints @  
<http://www.wright.edu/~nikolai.priezjev/>



- N. V. Priezjev, Accelerated relaxation in disordered solids under cyclic loading with alternating shear orientation, *J. Non-Cryst. Solids* **525**, 119683 (2019).
- N. V. Priezjev, The effect of cryogenic thermal cycling on aging, rejuvenation, and mechanical properties of metallic glasses, *J. Non-Cryst. Solids* **503**, 131 (2019).

# Outline

- Brief introduction (metallic glasses, amorphous structure, mechanical properties, etc)
- Part I: Cyclic loading with alternating shear orientation (“*mechanical annealing*”)

N. V. Priezjev, Accelerated relaxation in disordered solids under cyclic loading with alternating shear orientation, *J. Non-Cryst. Solids* **525**, 119683 (2019).

- Part II: Cryogenic thermal cycling and mechanical properties of metallic glasses

N. V. Priezjev, The effect of cryogenic thermal cycling on aging, rejuvenation, and mechanical properties of metallic glasses, *J. Non-Cryst. Solids* **503**, 131 (2019).

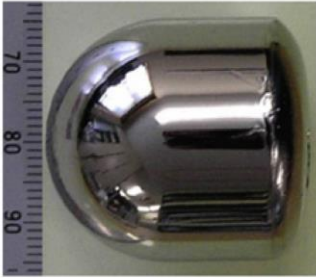
- Part III: Aging and rejuvenation during elastostatic loading of amorphous alloys

N. V. Priezjev, Aging and rejuvenation during elastostatic loading of amorphous alloys: A molecular dynamics simulation study, *Comput. Mater. Sci.* **168**, 125 (2019).

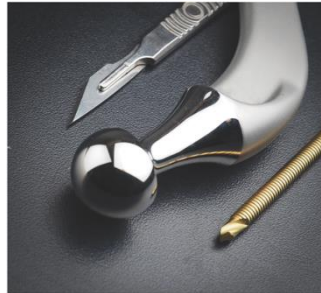
- Conclusions

# Amorphous structure, dynamical heterogeneity, and shear transformations

Metallic glasses: multicomponent alloys; high strength and elastic limit but low ductility



Cu-Zr-Al-Ag; ~30mm  
Inoue & Takeuchi (2011)



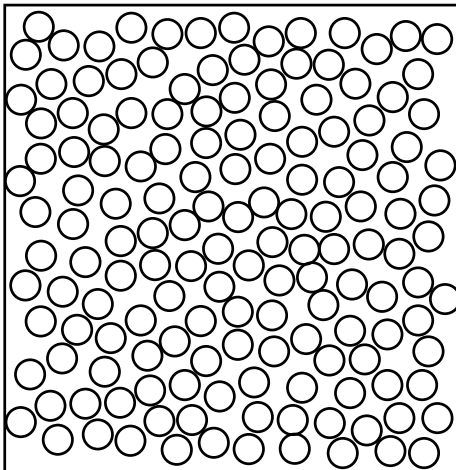
Biocompatible: Implantable medical  
devices and surgical tools (Mg-based)



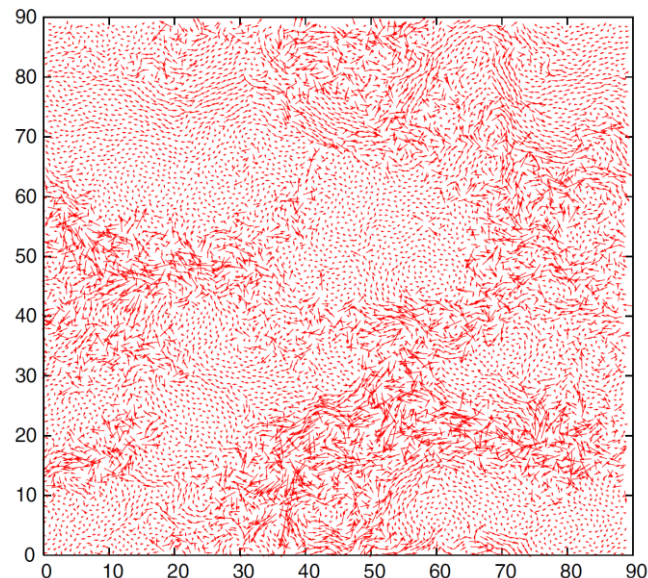
Wear, corrosion  
resistant



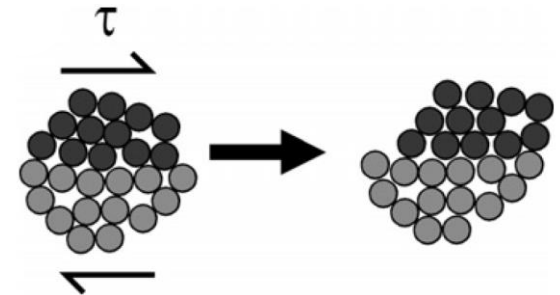
Sporting goods:  
*e.g.*, golf clubs



Disordered structure;  
no long-range order



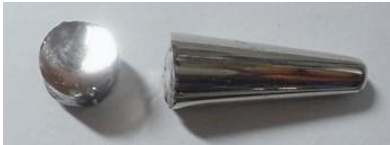
Spatial map of single-particle dis-  
placements, Berthier & Biroli (2011)



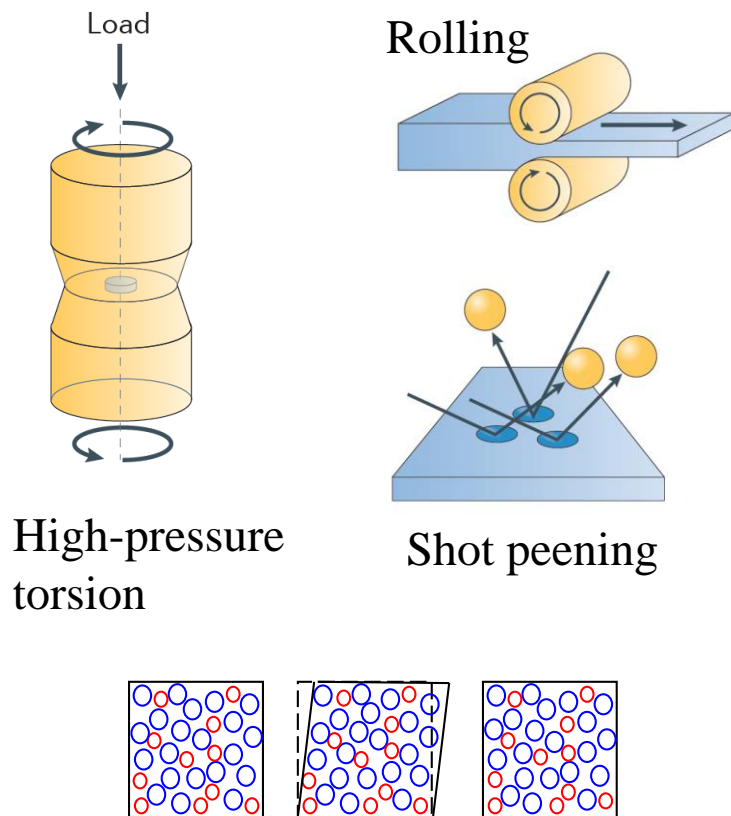
Localized shear transformations  
Spaepen (1977) & Argon (1979)

# Thermomechanical processing: Structural relaxation and rejuvenation

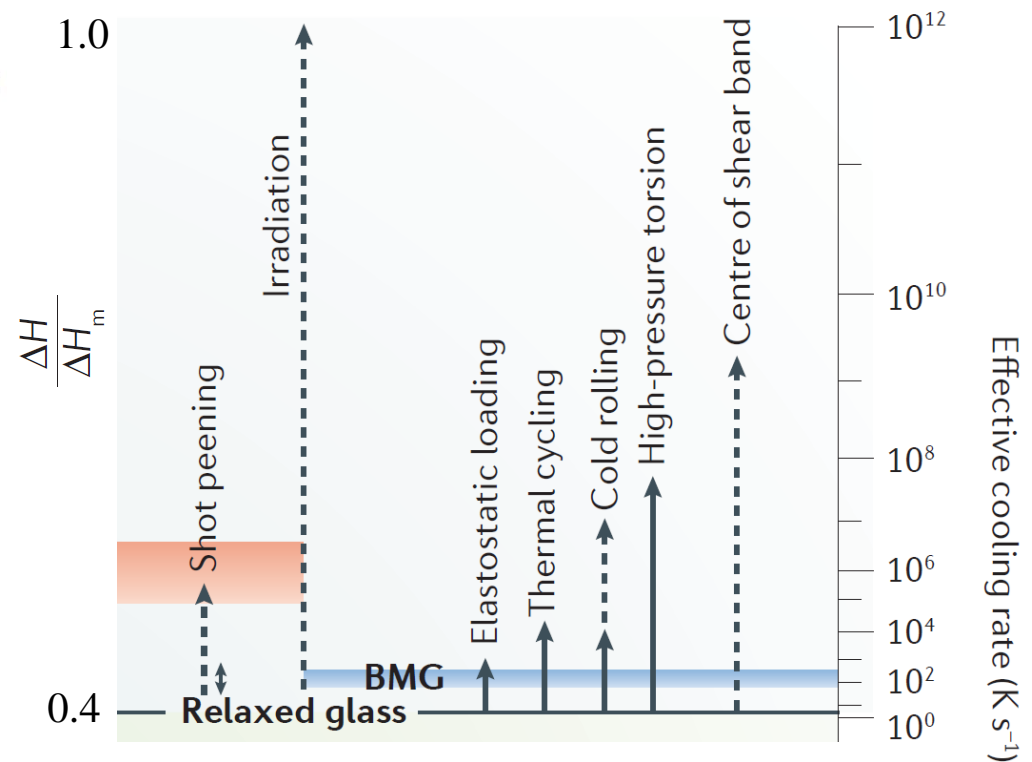
Metallic glasses: mechanical properties include high strength and low ductility (brittle)



Sun, Concustell, and Greer, Thermomechanical processing of metallic glasses: extending the range of the glassy state, *Nature Reviews Materials* **1**, 16039 (2016).



## Rejuvenation: increase in stored energy

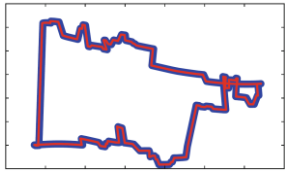


Relaxation: (1) cyclic loading or “*mechanical annealing*”, (2) ultrastable glasses by deposition

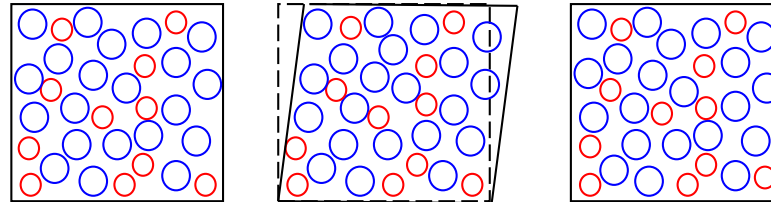


# Part I: Cyclic loading with alternating shear orientation ( “mechanical annealing” )

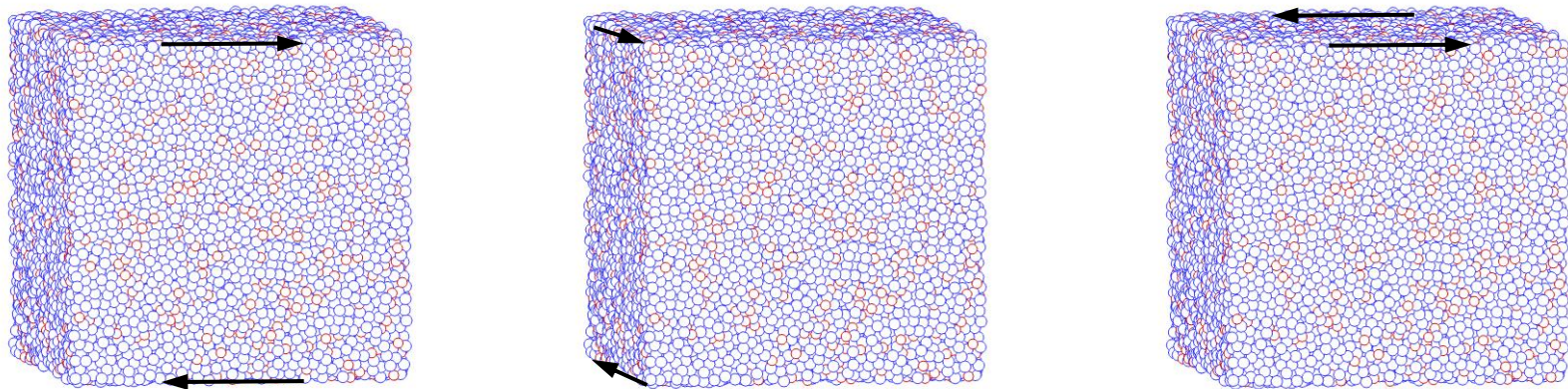
2 cycles at  $T=0$



Regev *et al.* 2015



Periodic shear; one plane  
Priezjev *JNCS* (2018)  
Sastry *et al.* (2017)



N. V. Priezjev, Accelerated relaxation in disordered solids under cyclic loading with alternating shear orientation, *J. Non-Cryst. Solids* **525**, 119683 (2019).

# Details of molecular dynamics simulations and parameter values

Binary Lennard-Jones Kob-Andersen mixture:

$$V_{LJ}(r) = 4\epsilon_{\alpha\beta} \left[ \left( \frac{\sigma_{\alpha\beta}}{r} \right)^{12} - \left( \frac{\sigma_{\alpha\beta}}{r} \right)^6 \right] \quad \text{Ni}_{80}\text{P}_{20}$$

Parameters for  $\alpha\beta = A$  and  $B$  particles:

$$\epsilon_{AA} = 1.0, \epsilon_{AB} = 1.5, \epsilon_{BB} = 0.5, m_A = m_B$$

$$\sigma_{AA} = 1.0, \sigma_{AB} = 0.8, \sigma_{BB} = 0.88$$

$$\text{Monomer density: } \rho = \rho_A + \rho_B = 1.20 \sigma^{-3}$$

$$\text{Temperature: } T_{LJ} = 0.01 \epsilon/k_B \ll T_g = 0.435 \epsilon/k_B$$

$$\text{System size: } L = 36.84 \sigma, N_p = 60000$$

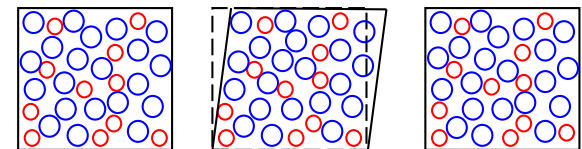
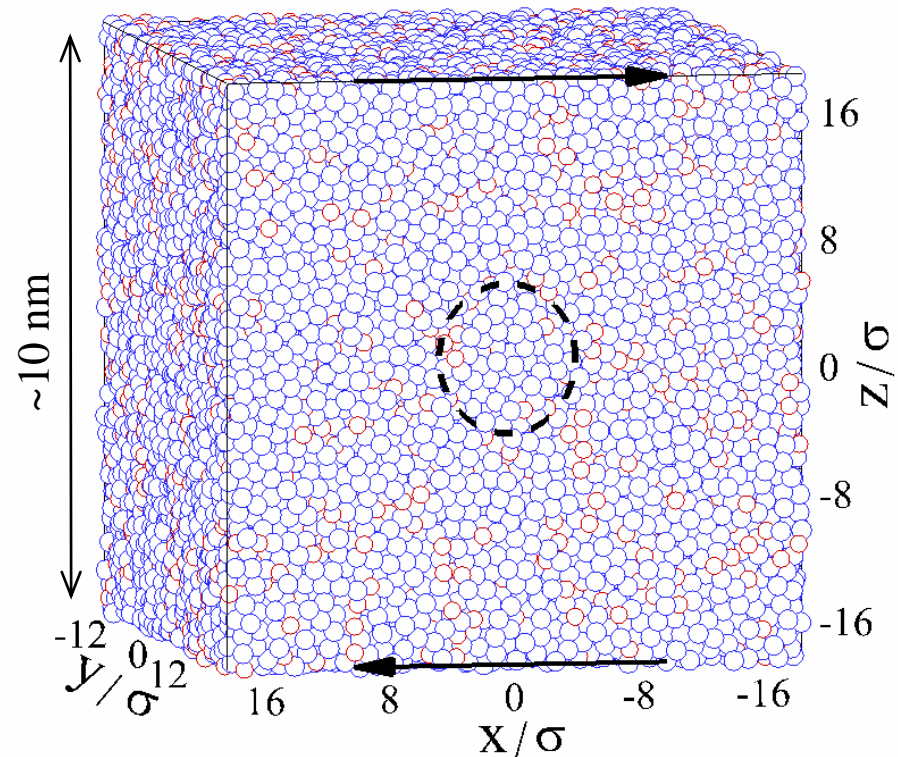
Lees-Edwards periodic boundary conditions

LAMMPS, Nose-Hoover thermostat,  $\Delta t_{MD} = 0.005 \tau$

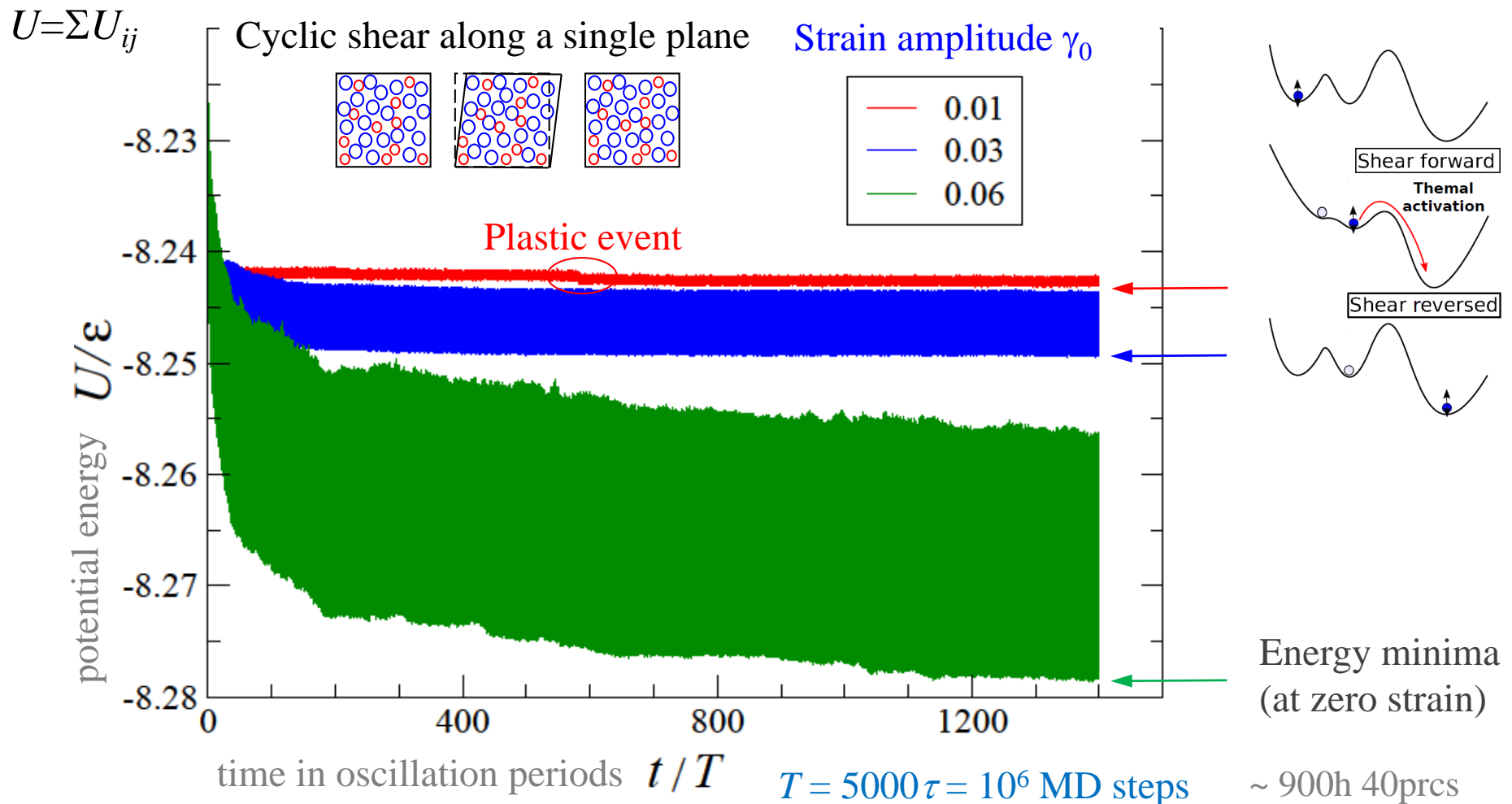
Fast annealing rate:  $10^{-2} \epsilon/k_B \tau$  (**poorly annealed glass**)  
**higher energy sample**

Oscillatory shear strain:  $\gamma(t) = \gamma_0 \sin(\omega t)$

Oscillation period:  $T = 2\pi / \omega = 5000 \tau$

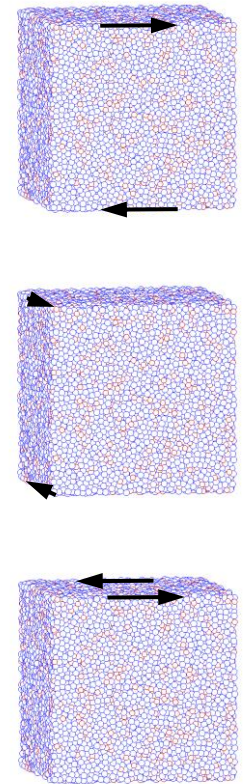
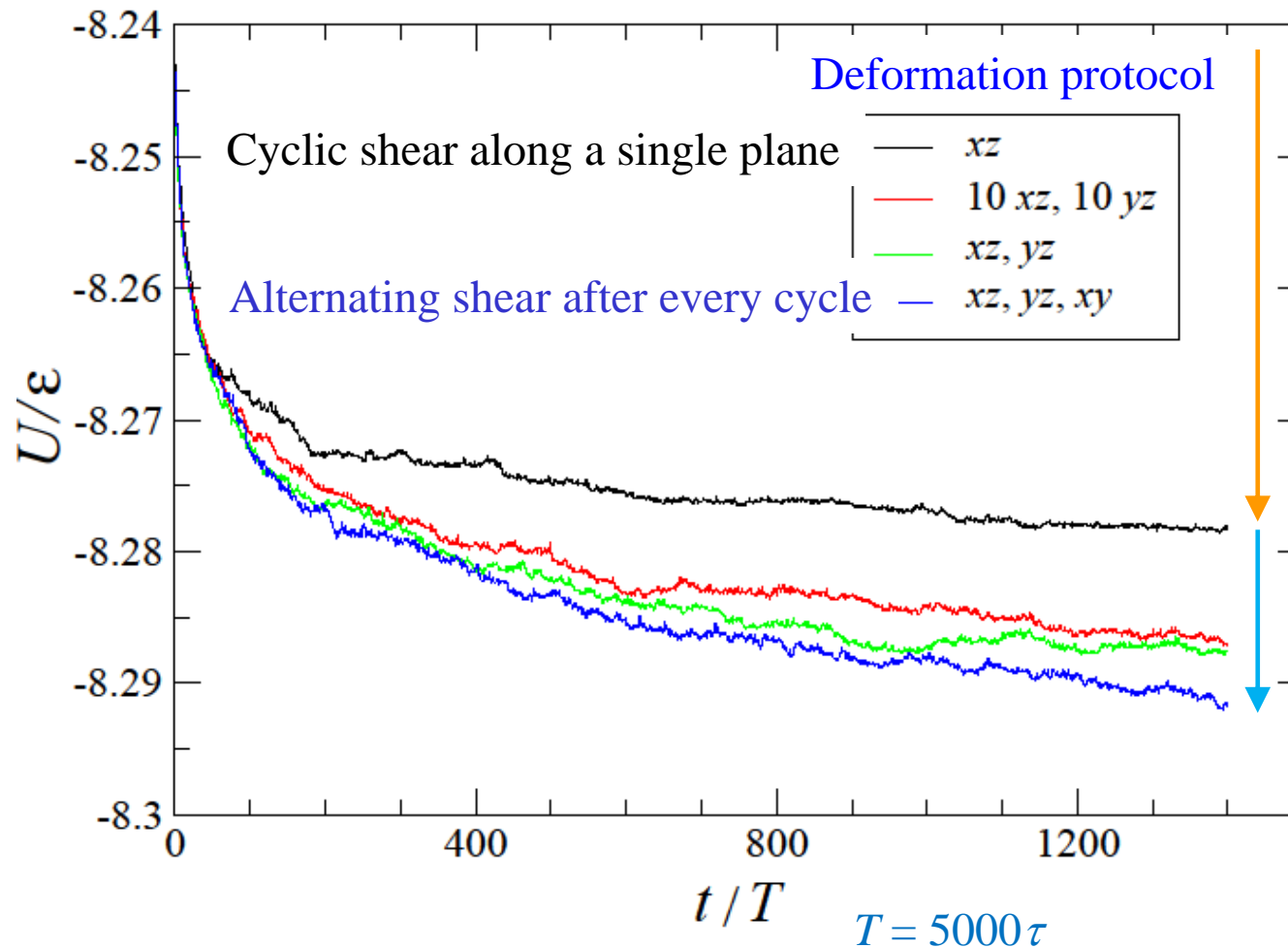


# Potential energy per particle $U$ during 1400 oscillation cycles for different $\gamma_0$



With increasing strain amplitude  $\gamma_0$  (below yield strain), the system relocates to deeper energy minima (via collective rearrangements of atoms).

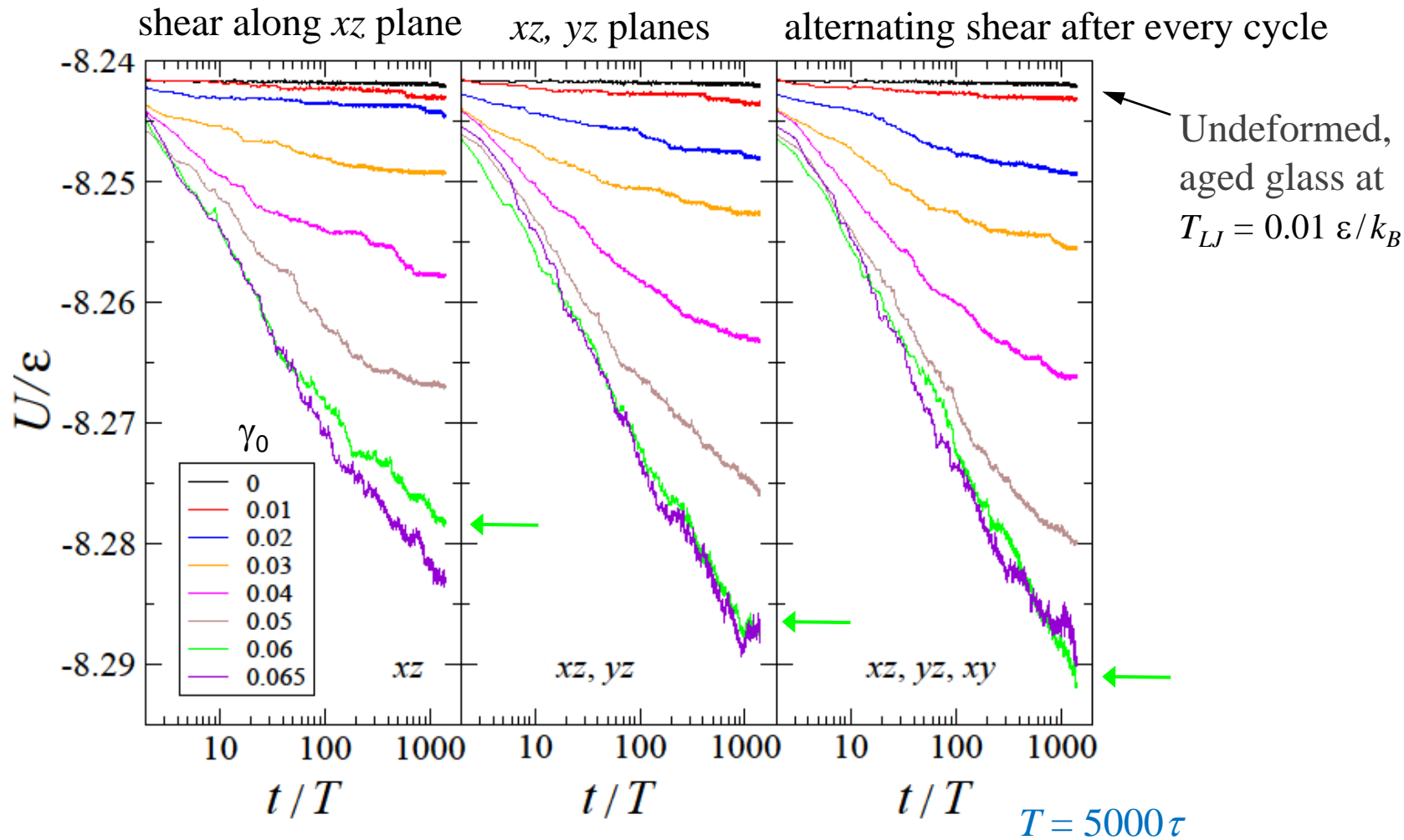
# Potential energy minima during 4 different deformation protocols for $\gamma_0 = 0.06$



For the strain amplitude  $\gamma_0 = 0.06$  (just below yield strain), each additional alternation of the shear orientation in the deformation protocol results in lower energy states.

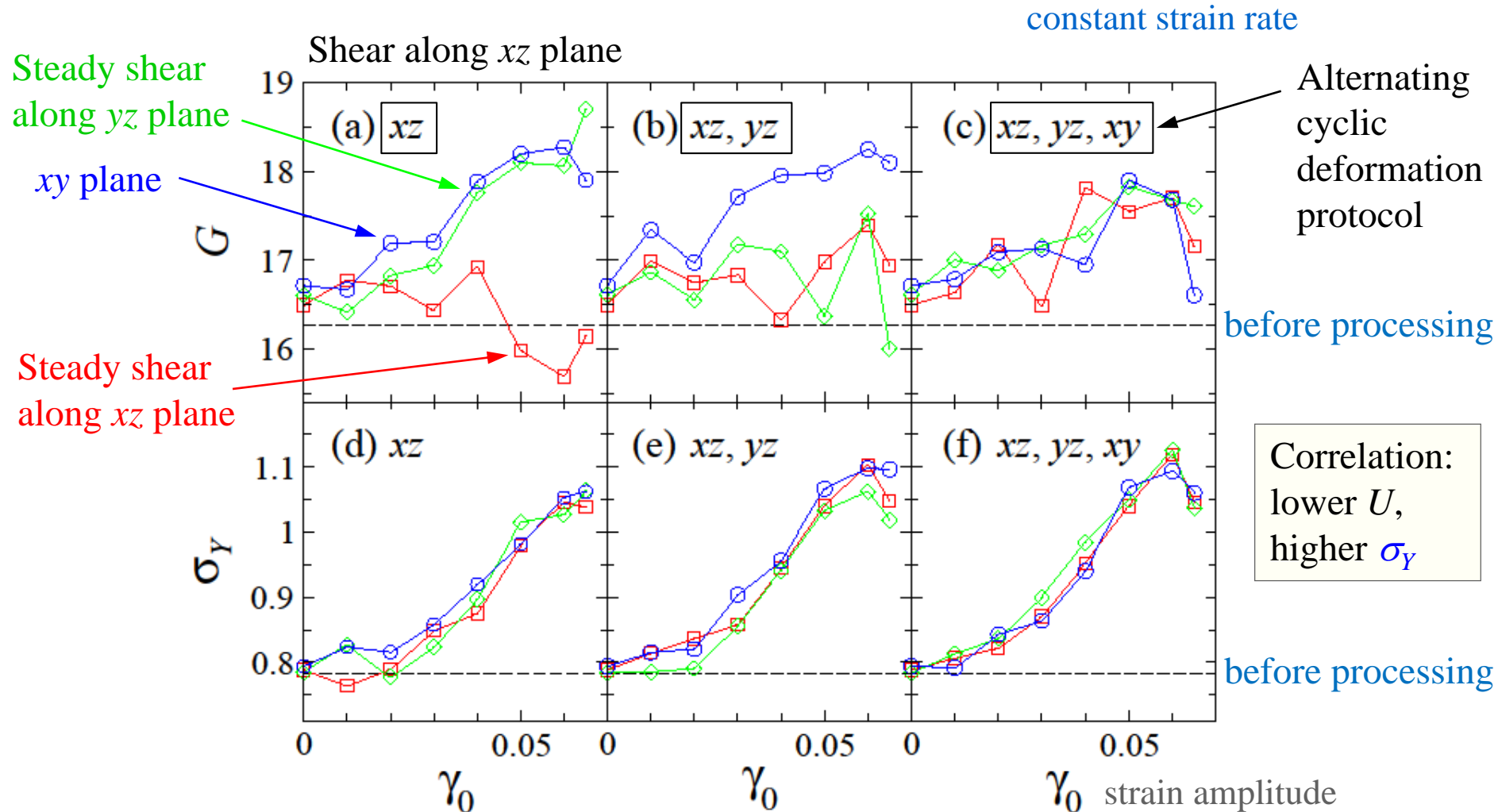


The potential energy  $U$  during 3 deformation protocols for the indicated  $\gamma_0$



For strain amplitudes  $\gamma_0$  (below yield strain), each additional alternation of the shear orientation in the deformation protocol results in lower energy states.

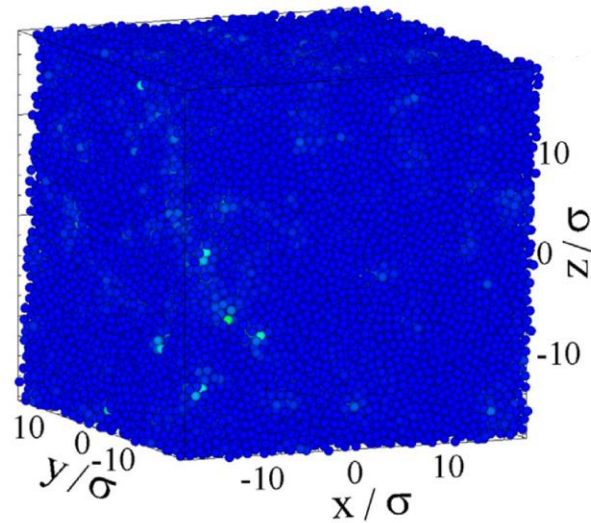
# Shear modulus $G$ and yielding peak $\sigma_Y$ during startup shear deformation



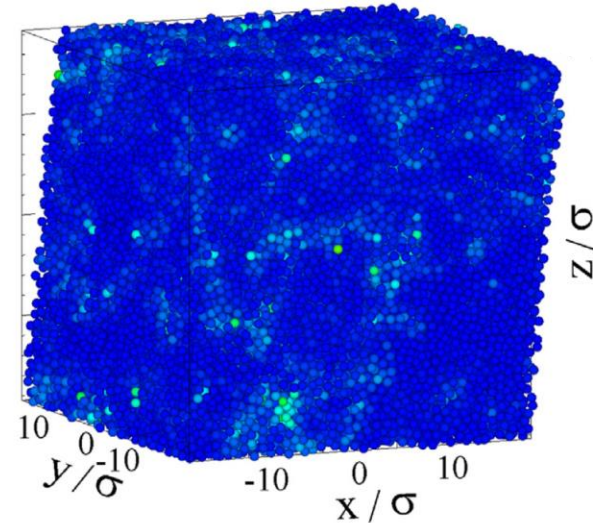
The height of the yielding peak  $\sigma_Y$  increases when an additional shear orientation is introduced in the cyclic loading protocol. The shear modulus  $G$  is larger along the shear directions that were not used during cyclic deformation.

# Snapshots of the strained glass after aging during 1400 T (no cyclic loading)

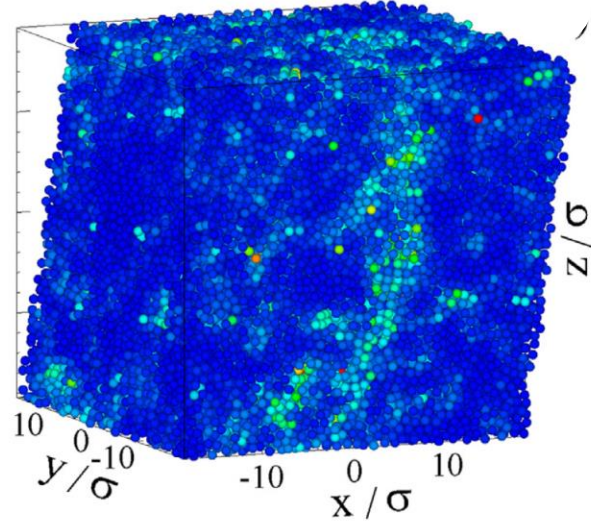
5% shear strain



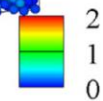
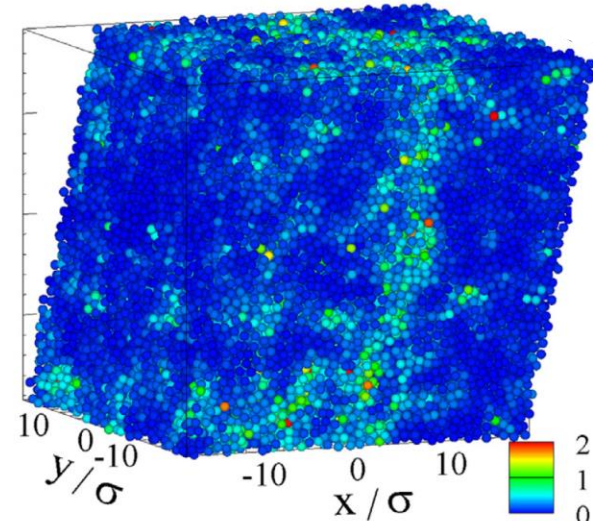
10% shear strain



15% shear strain



20% shear strain

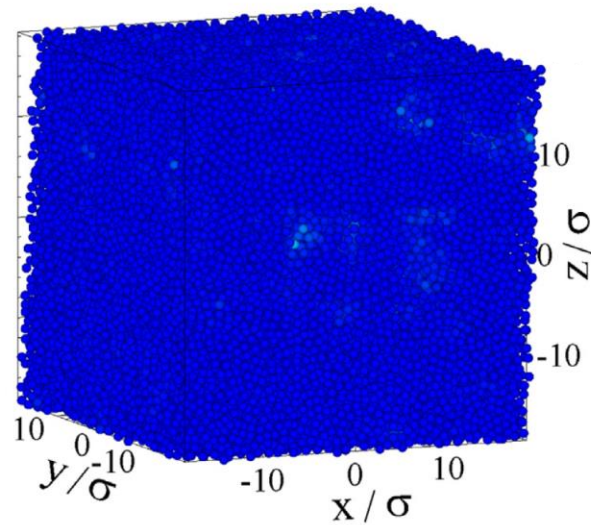


nonaffine  
measure  $D^2$

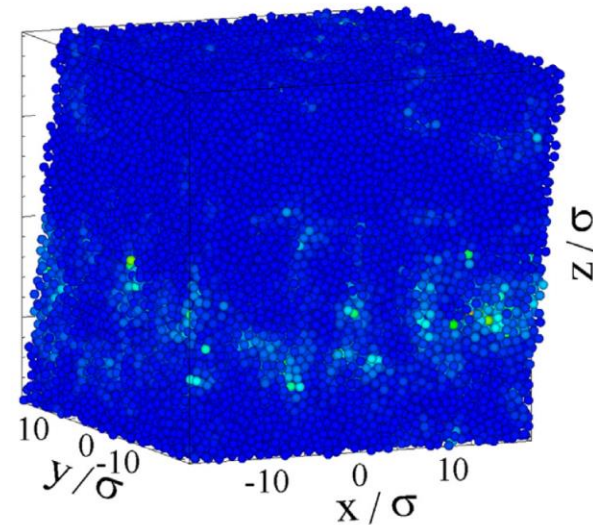


# Snapshots of strained glass after 1400 alternating shear cycles (xz, yz, xy)

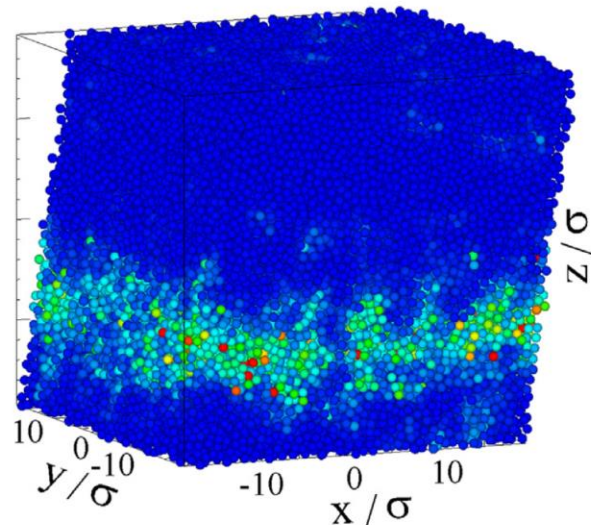
5% shear strain



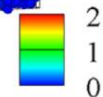
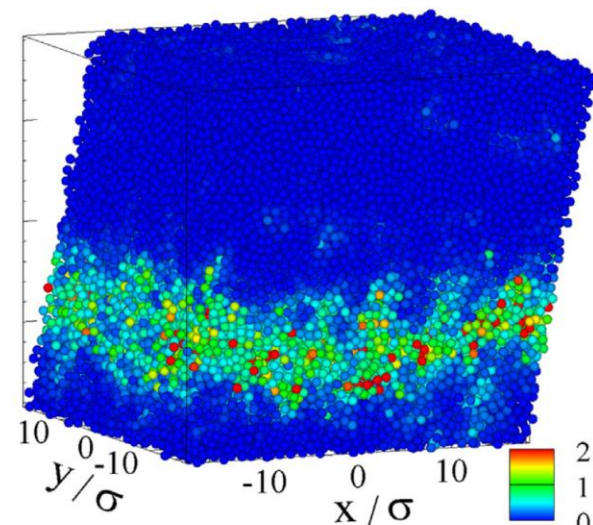
10% shear strain



15% shear strain

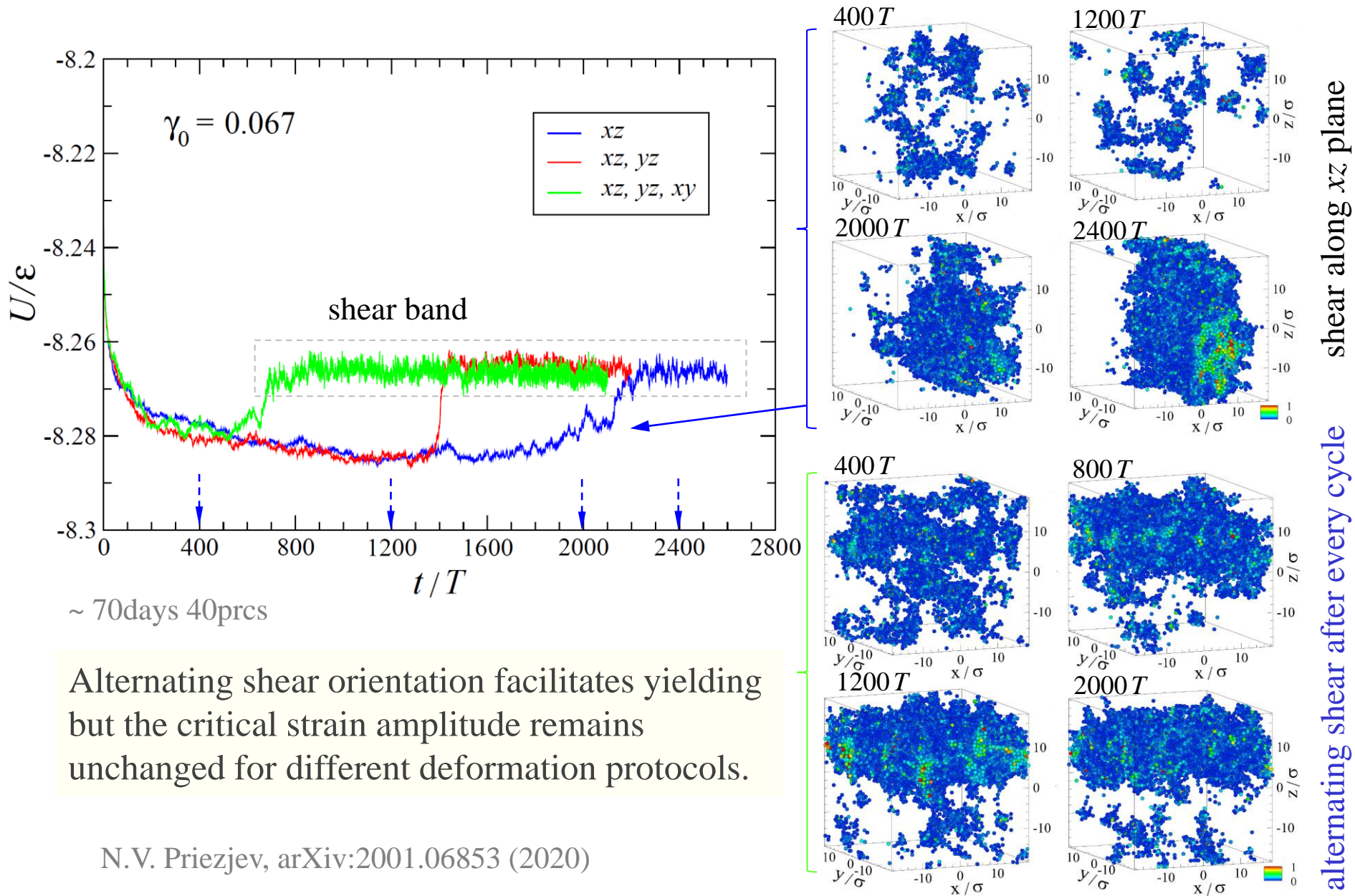


20% shear strain



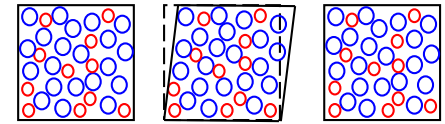
nonaffine  
measure  $D^2$

# Yielding transition and shear band at the critical strain amplitude $\gamma_0=0.067$





## Conclusions:

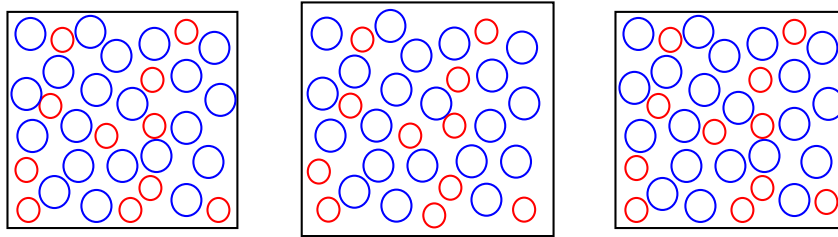


2400 shear cycles

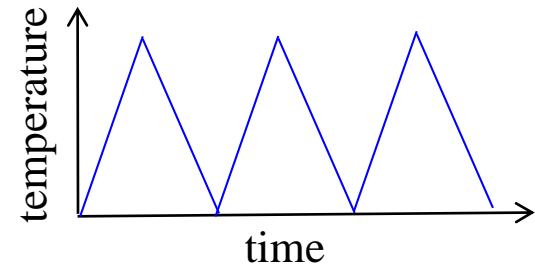
- Periodic shear deformation (in the “elastic” range) leads to relaxed, lower energy states ( “*mechanical annealing*” ).
- For a fixed strain amplitude (below yield strain), each additional alternation of the shear orientation in the deformation protocol results in lower energy states.
- The yielding peak increases in glasses deformed at higher strain amplitudes.
- The shear modulus is larger along the shear directions that were not cyclically loaded.

N. V. Priezjev, Accelerated relaxation in disordered solids under cyclic loading with alternating shear orientation, *J. Non-Cryst. Solids* **525**, 119683 (2019).

## Part II: The effect of cryogenic thermal cycling on potential energy states and mechanical properties of metallic glasses



100 thermal cycles



Ketov, Sun, Nachum, Lu, Checchi, Beraldin, Bai, Wang, Louzguine-Luzgin, Carpenter, and Greer, **Rejuvenation of metallic glasses by non-affine thermal strain**, *Nature* **524**, 200 (2015).

Shang, Guan, and Barrat, Role of thermal expansion heterogeneity in the cryogenic rejuvenation of metallic glasses, *J. Phys.: Mater.* **1**, 015001 (2018).

Priezjev, The effect of cryogenic thermal cycling on aging, rejuvenation, and mechanical properties of metallic glasses, *J. Non-Cryst. Solids* **503**, 131 (2019).

# Details of molecular dynamics simulations and parameter values

Binary Lennard-Jones Kob-Andersen mixture:

$$V_{LJ}(r) = 4\epsilon_{\alpha\beta} \left[ \left( \frac{\sigma_{\alpha\beta}}{r} \right)^{12} - \left( \frac{\sigma_{\alpha\beta}}{r} \right)^6 \right] \quad \text{Ni}_{80}\text{P}_{20}$$

Parameters for  $\alpha, \beta = A$  and  $B$  particles:

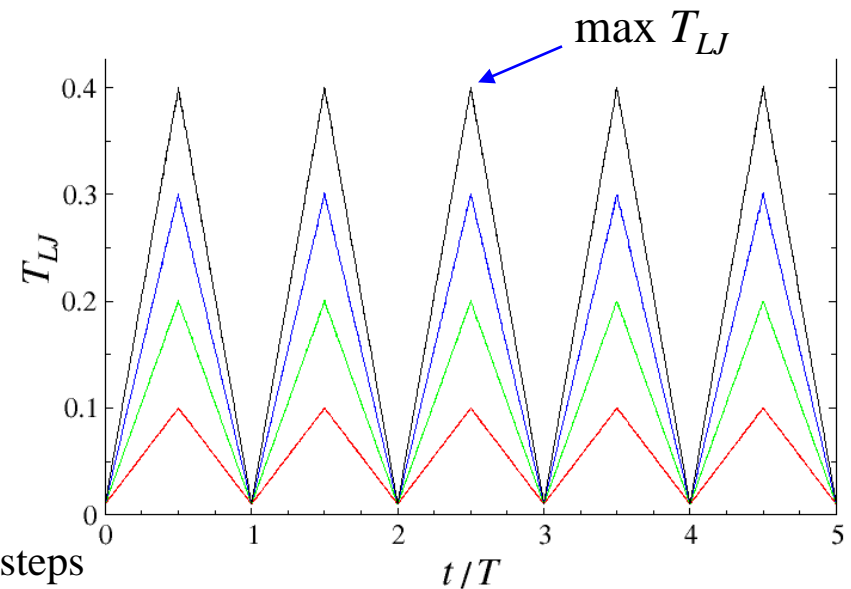
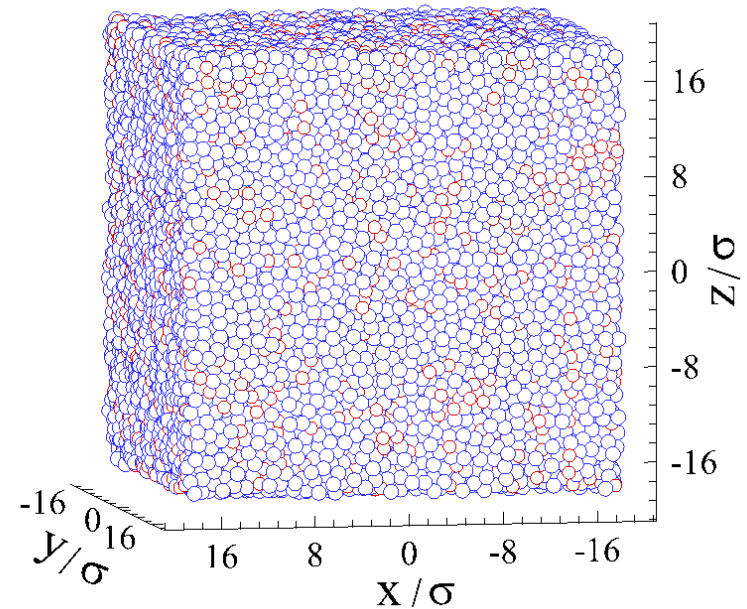
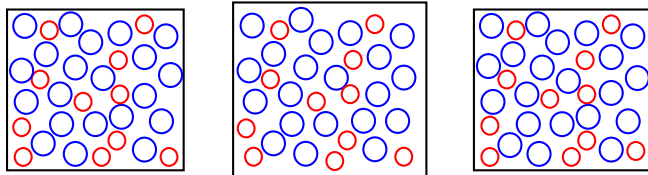
$$\epsilon_{AA} = 1.0, \epsilon_{AB} = 1.5, \epsilon_{BB} = 0.5, m_A = m_B$$

$$\sigma_{AA} = 1.0, \sigma_{AB} = 0.8, \sigma_{BB} = 0.88$$

Temperature:  $T_{LJ} = 0.01 \epsilon/k_B < T_g \approx 0.35 \epsilon/k_B$

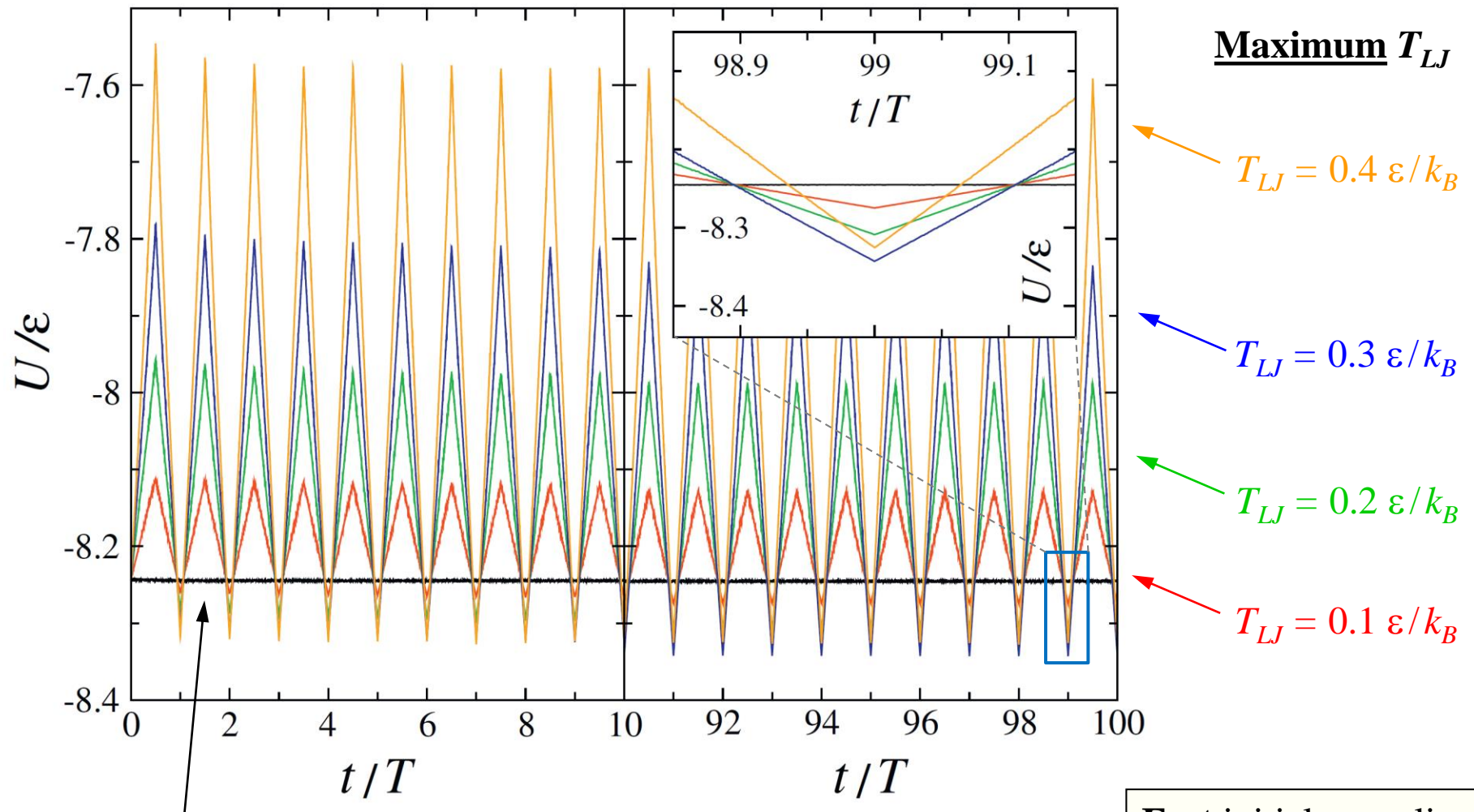
LAMMPS:  $N_p = 60000$ , MD step  $\Delta t_{MD} = 0.005 \tau$

Initial quench rates:  $10^{-2} \epsilon/k_B \tau$  to  $10^{-5} \epsilon/k_B \tau$



Pressure  $P = 0$  and thermal period  $T = 5000\tau = 10^6$  MD steps

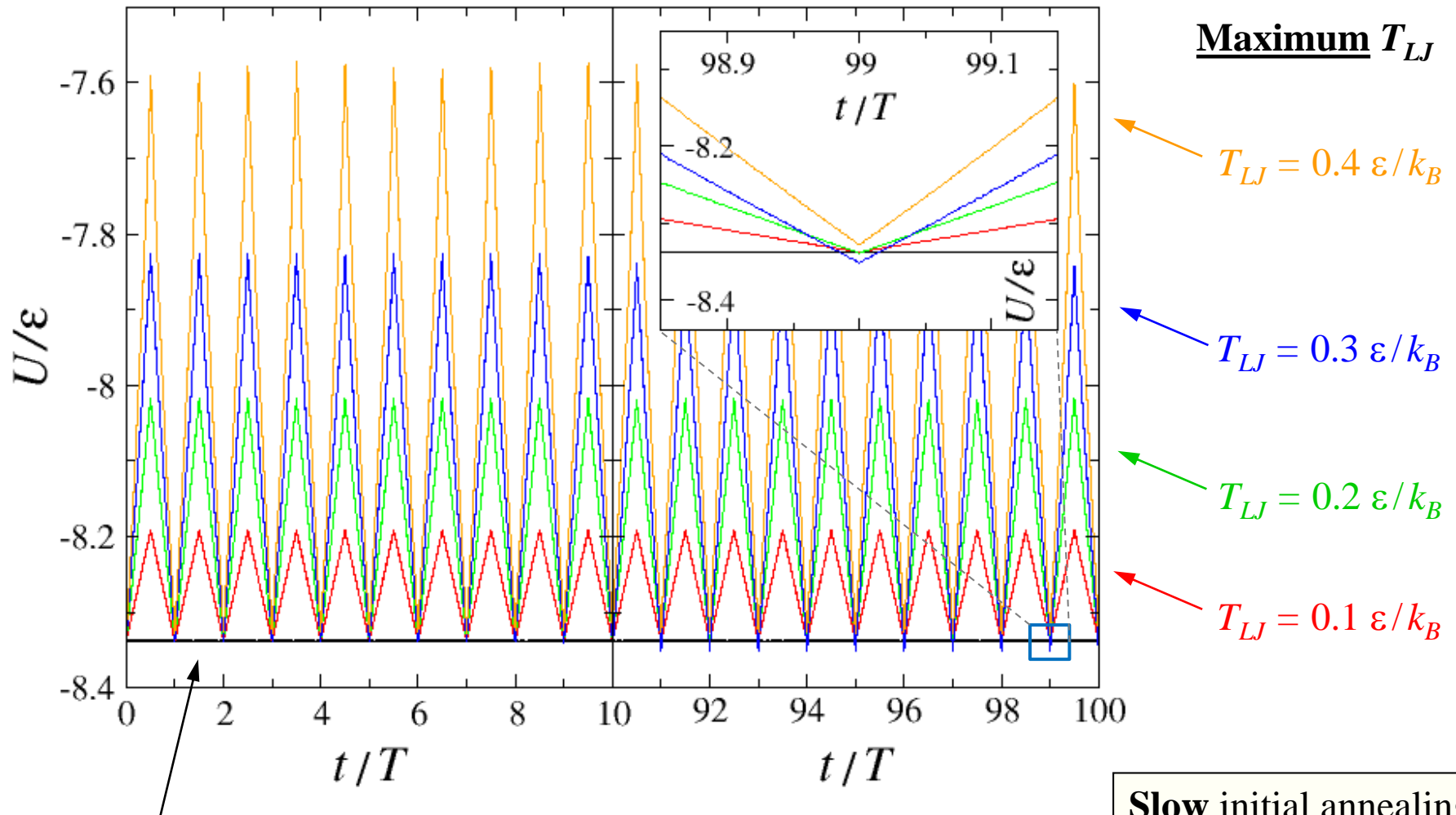
# Potential energy per atom during 100 thermal cycles for different max $T_{LJ}$



Aging at constant temperature:  $T_{LJ} = 0.01 \epsilon/k_B$

**Fast initial annealing**  
rate:  $10^{-2} \epsilon/k_B \tau$ ,  
**poorly-annealed glass**

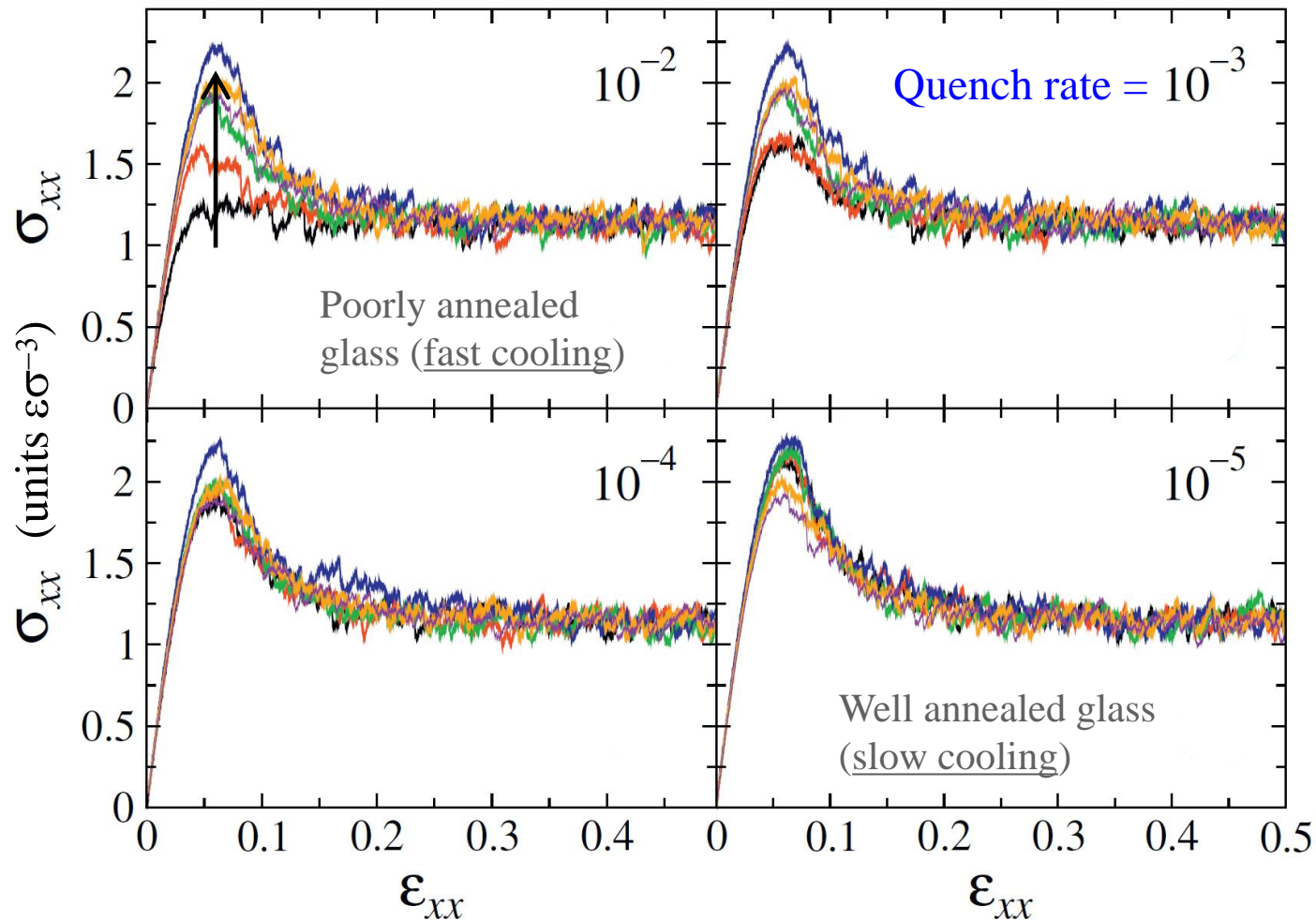
# Potential energy per atom during 100 thermal cycles for different max $T_{LJ}$



Aging at constant temperature:  $T_{LJ} = 0.01 \epsilon/k_B$



# Tensile stress vs strain after 100 cycles: effects of quench rate and max $T_{LJ}$



**Maximum  $T_{LJ}$**

$$T_{LJ} = 0.4 \epsilon/k_B$$

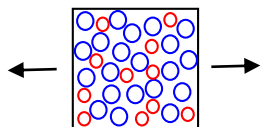
$$T_{LJ} = 0.30 \epsilon/k_B$$

$$T_{LJ} = 0.2 \epsilon/k_B$$

$$T_{LJ} = 0.1 \epsilon/k_B$$

$$T_{LJ} = 0.01 \epsilon/k_B$$

Aged glasses

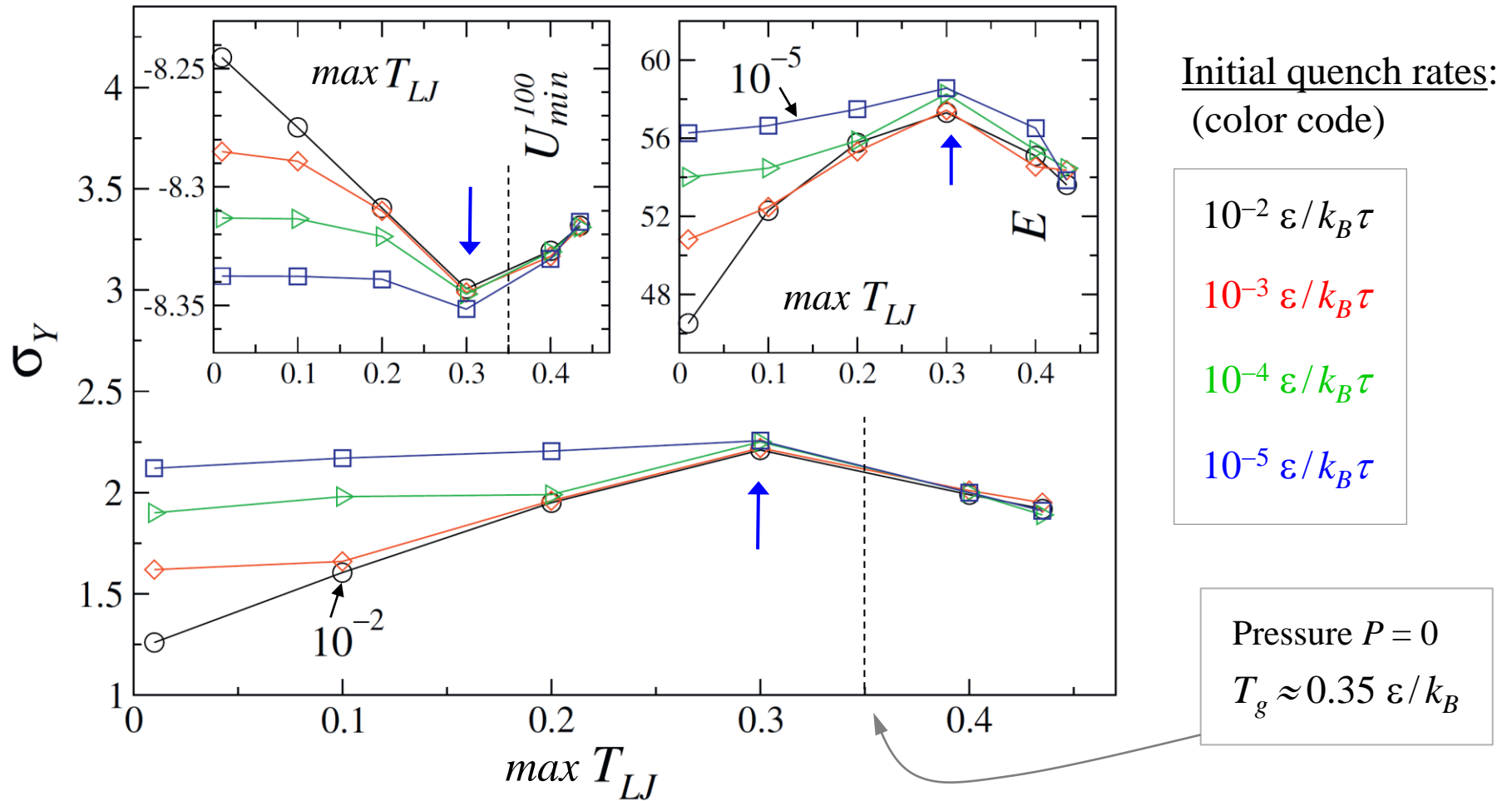


Aged glasses (black curves): higher yield peak at slower quench rates

Strain rate =  $10^{-5} 1/\tau$

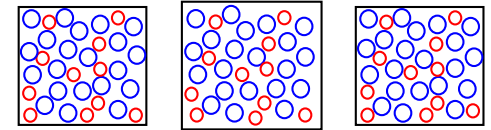
Highest yield peak (blue curves) at maximum  $T_{LJ} = 0.30 \epsilon/k_B$

# The yielding peak $\sigma_Y$ , elastic modulus $E$ , and $U_{min}$ versus maximum $T_{LJ}$



- Highest yield peak and elastic modulus after thermal loading with maximum  $T_{LJ} = 0.30 \epsilon/k_B$
- A correlation between minimum potential energy  $U_{min}$  and maximum values of  $\sigma_Y$  and  $E$ .

## Conclusions:

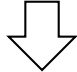


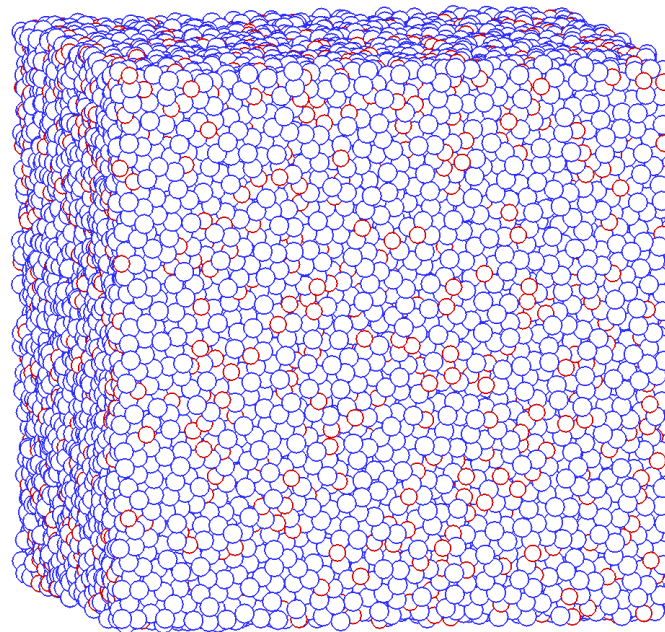
100 thermal cycles

- MD simulations of binary 3D Lennard-Jones glasses that are initially prepared with different cooling rates and then subjected to repeated cycles of heating and cooling.
- The potential energy in rapidly annealed glasses decreases during thermal cycling, while the energy in slowly annealed glasses increases at large cycling amplitudes ( $>T_g$ ).
- The elastic modulus and the yielding peak (after the thermal treatment) acquire maximum values at a particular  $\max T_{LJ}$  which coincides with the minimum of the potential energy.

N. V. Priezjev, The effect of cryogenic thermal cycling on aging, rejuvenation, and mechanical properties of metallic glasses, *Journal of Non-Crystalline Solids* **503-504**, 131-138 (2019).

## Part III: Aging and rejuvenation during elastostatic loading of amorphous alloys

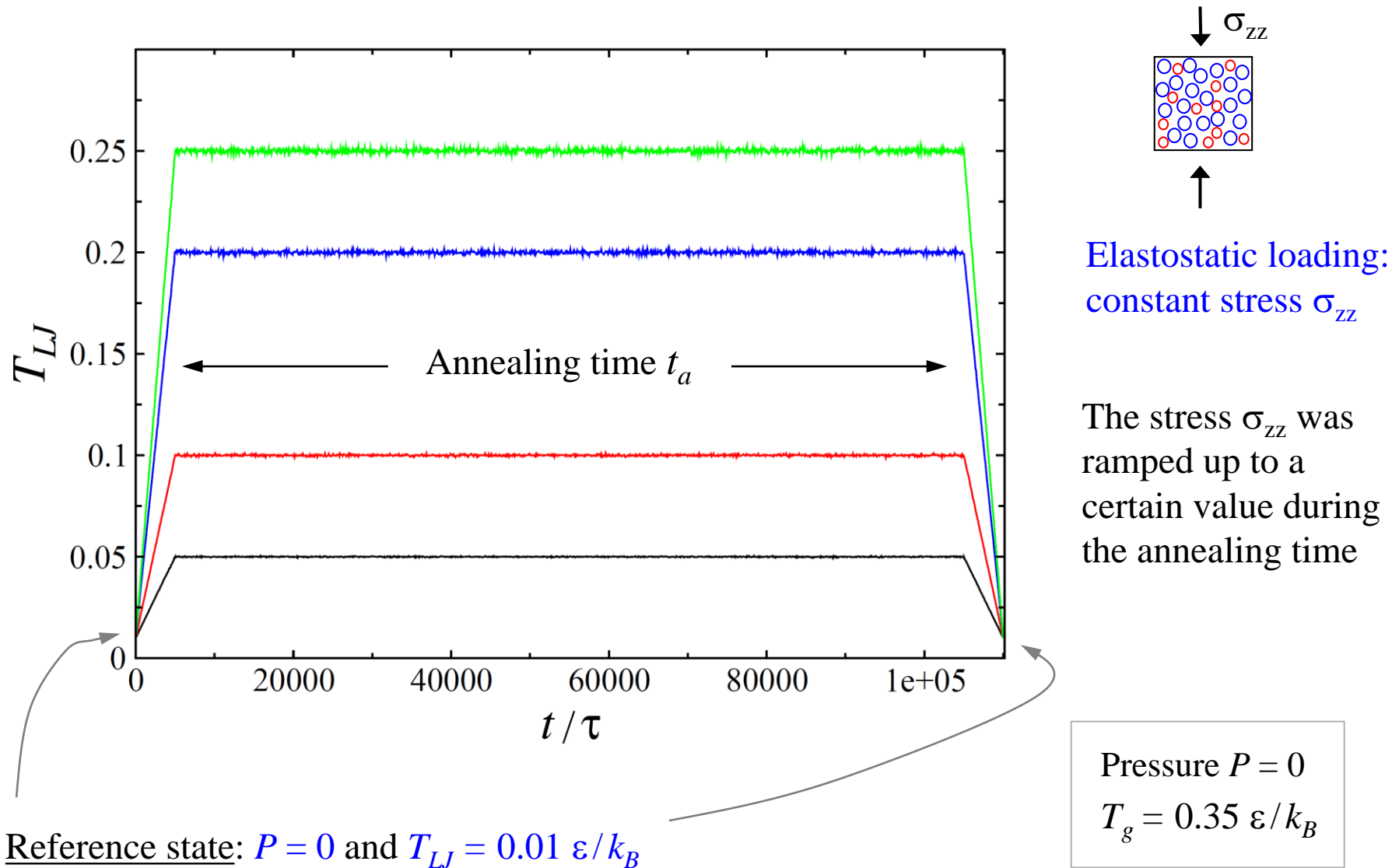
Constant applied stress  $\sigma_{zz}$  



At what stress, temperature to load, and for how long?

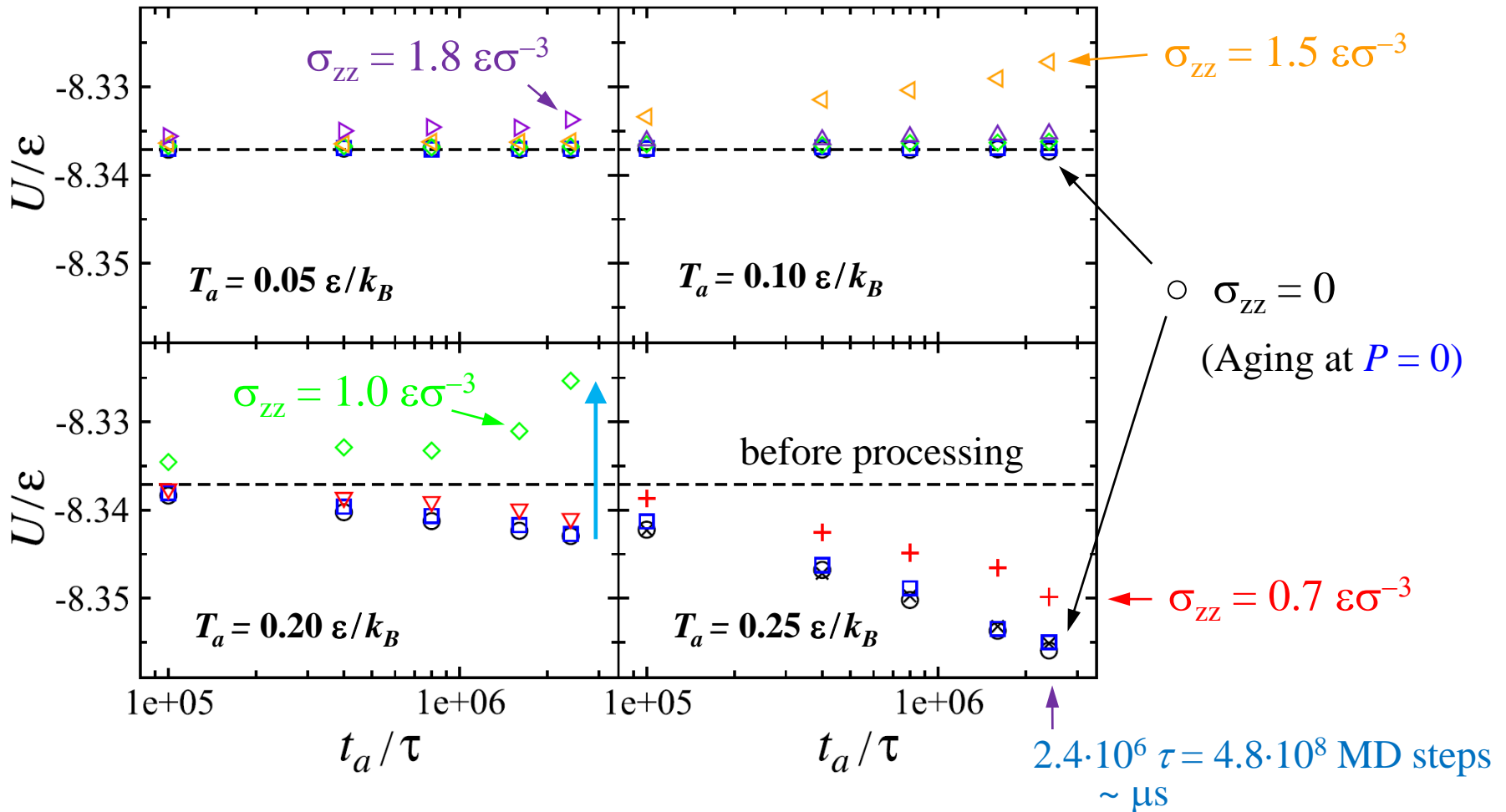
N. V. Priezjev, Aging and rejuvenation during elastostatic loading of amorphous alloys: A molecular dynamics simulation study, *Comput. Mater. Sci.* **168**, 125 (2019).

# Setup: Temperature profiles, annealing time, glass transition temperature





# Variation of the potential energy vs. annealing time at different temp $T_a$

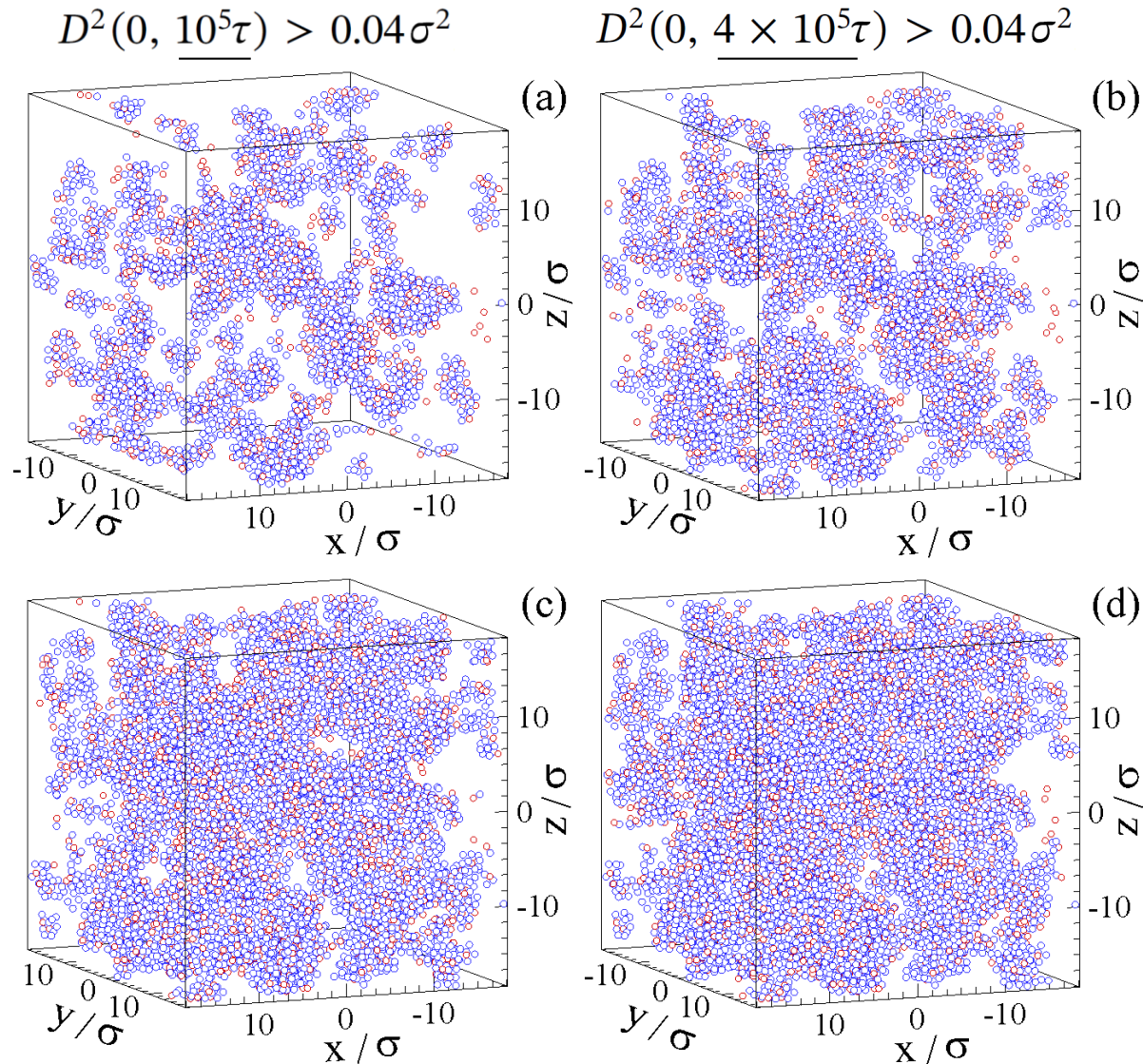


Constant applied stress  $\sigma_{zz}$  is up to  $\sim 70$ - $80\%$  of the yielding peak at a given temperature  $T_a$

Aging: high  $T_a < T_g = 0.35 \epsilon/k_B$  and low stress  $\sigma_{zz}$       Rejuvenation: low  $T_a$  and high  $\sigma_{zz}$

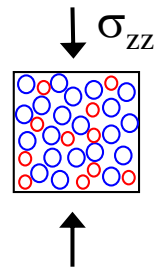
# Collective nonaffine displacements vs. annealing time at $T_a = 0.1 \epsilon/k_B$

Empty regions correspond to atoms that remained in their cages during the annealing time

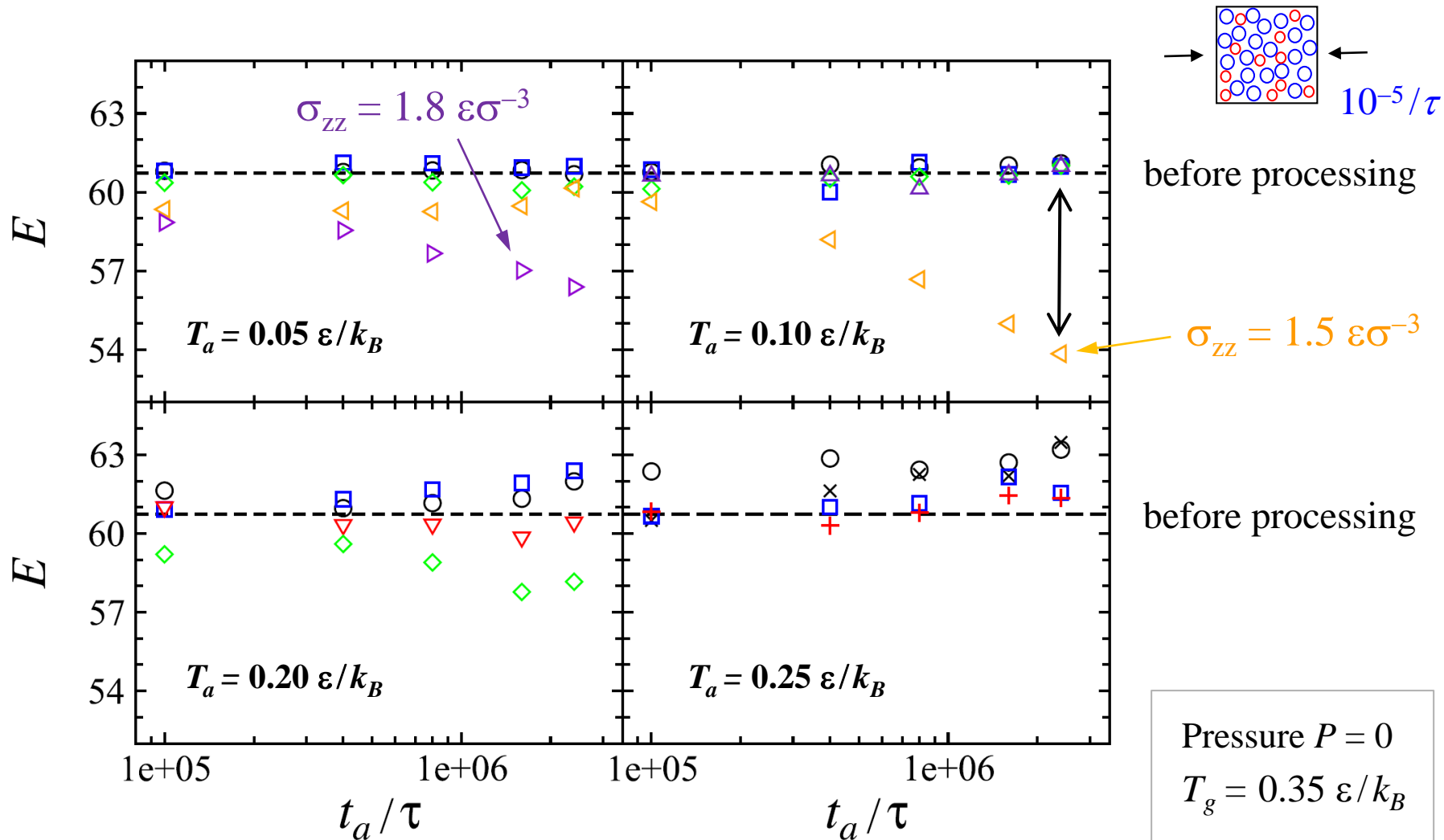


Elastostatic loading:  
constant applied stress:

$$\sigma_{zz} = 1.5 \epsilon \sigma^{-3}$$



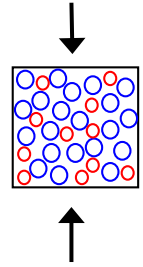
The elastic modulus  $E$  vs. annealing time  $t_a$  at different temperatures  $T_a$



Maximum effect of rejuvenation due to elastostatic loading: about 10% decrease in  $E$

## Conclusions:

Elastostatic loading:  
constant stress  $\sigma_{zz}$



- Well-annealed binary glass at zero pressure is elastostatically loaded during extended time intervals ( $\sim 10^8$  MD steps) in a wide range of annealing temperatures.
- Annealing: high  $T_a < T_g = 0.35 \varepsilon/k_B$  and low stress  $\sigma_{zz}$       Rejuvenation: low  $T_a$  and high  $\sigma_{zz}$   
 $T_a < 0.6 T_g$        $\sigma_{zz} \approx 0.8 \sigma_Y$
- Maximum effect of rejuvenation due to elastostatic loading: about 10% decrease in  $E$

N. V. Priezjev, Aging and rejuvenation during elastostatic loading of amorphous alloys:  
A molecular dynamics simulation study, *Comput. Mater. Sci.* **168**, 125 (2019).